THE JOURNAL OF PHYSICAL CHEMISTRY B

Article

pubs.acs.org/JPCB

Thermodynamic Study of Rhodamine 123-Calf Thymus DNA Interaction: Determination of Calorimetric Enthalpy by Optical Melting Study

Abdulla Al Masum,[†] Maharudra Chakraborty,[‡] Prateek Pandya,[§,∥] Umesh Chandra Halder,[‡] Md. Maidul Islam,*[,†] and Subrata Mukhopadhyay[‡]

[†]Department of Chemistry, Aliah University, Sector V, Salt Lake City, Kolkata 700 091, India

[‡]Department of Chemistry, Jadavpur University, Kolkata 700 032, India

[§]Department of Chemistry, University of Rajasthan, Jaipur 302 004, India

Supporting Information

ABSTRACT: In this paper, the interaction of rhodamine123 (R123) with calf thymus DNA has been studied using molecular modeling and other biophysical methods like UV−vis spectroscopy, fluorometry, optical melting, isothermal titration calorimetry, and circular dichroic studies. Results showed that the binding energy is about −6 to −8 kcal/mol, and the binding process is favored by both negative enthalpy change and positive entropy change. A new method to determine different thermodynamic properties like calorimetric enthalpy and heat capacity change has been introduced in this paper. The obtained data has been crossed-checked by other methods. After dissecting the free-energy contribution, it was observed that the binding was favored by both negative hydrophobic free energy and negative molecular free energy which compensated for the positive free energies due to the conformational change loss of rotational and transitional freedom of the DNA helix.

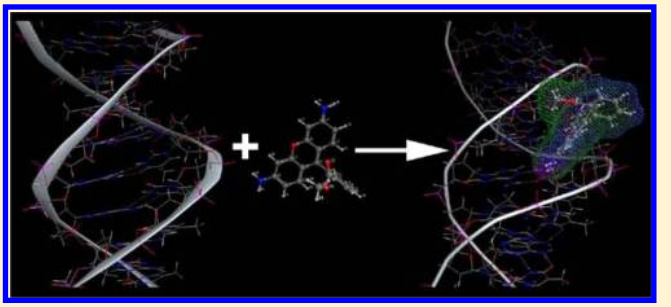

INTRODUCTION

Affinity of small molecules toward DNA has become an important topic of research. A lot of effort has been put in by various groups of researchers to find out new agents with novel therapeutic potential.[1−6] DNA binding agents are quite useful in a variety of diseases such as cancer, viral diseases, etc. However, a DNA binding agent can indiscriminately target healthy as well as cancerous cells. This problem can be dealt with by designing potent sequence-specific DNA binding agents that target only specific regions of DNA. In general, minor groove binders are known to interact with some degree of sequence specificity as compared to intercalators. A number of synthetic polyamides have been designed by Dervan and coworkers that target specific sequences of DNA duplexes.[7,8] In the quest for identifying target specific interactions, it is important to understand the molecular recognition signatures of small molecules with biomacromolecules.

Rhodamine 123 (Figure 1), a common dye from rhodamine family, is extensively used by researchers due to its various biological importance, such as inhibitor of mitochondrial function,[9,10] tracer membrane transport,[11−13] and antibacterial activity.[14] In vitro studies revealed that rhodamine 123 is toxic against different cell line[15] and reduces the growth of carcinoma cell.[16,17] The cytotoxicity and antimicrobial activity of rhodamine 123 may be due to affinity to DNA; however, DNA binding ability of rhodamine 123 has not yet been reported. In

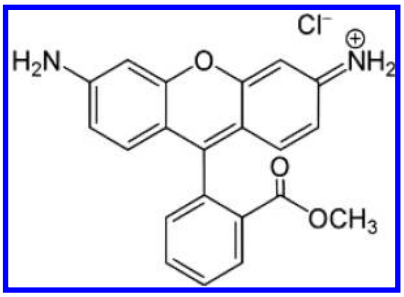

Figure 1. Structure of Rhodamine 123.

our present study, we have investigated the details mode, mechanism, and thermodynamic properties of binding of R123 to DNA. This work is motivated by our previous work,[18] where we studied the interaction of rhodamine B with CT DNA. Rhodamine B is a common food additive used in India and which is useful to know the probable effects of it on biological systems. We found rhodamine B strongly binds with CT DNA and may be hazardous to human health.[18] The affinity of rhodamine B to DNA motivated us to study thoroughly the

Received: September 15, 2014
Revised: October 19, 2014

   dx.doi.org/10.1021/jp509326r | J. Phys. Chem. B XXXX, XXX, XXX−XXX

bioactivity of other derivatives of rhodamine B to find out any difference between them in light of DNA interaction activity.

EXPERIMENTAL SECTION

Materials. CT DNA and Rhodamine 123 were purchased from Sigma-Aldrich Corporation (St. Louis, MO), and its concentration was determined spectrophotometrically. Known molar extinction coefficients of CT DNA (ε = 6600 M^{-1} cm^{-1} at 260 nm)[19] (expressed in terms of nucleotide phosphates) and rhodamine 123 (75000 M^{-1} cm^{-1} at 500 nm)[20] were used to determine the concentration by absorbance measurements. No deviation from Beer's law was observed in the concentration range at 0−100 μM for R123 used in our study.

Citrate-phosphate (CP) buffer medium (10 mM [Na^+]) of pH 7.0 containing 5.0 mM Na_2HPO_4 and suitable amount of citric acid was used in all the experiments.[21,22] The pH values of the solutions were measured with a calibrated Orion-Ross combined electrode system (model 81-02). All buffer solutions were filtered through Millipore filters (Millipore, India Pvt. Ltd., Bangalore, India) of 0.45 μM, before use.

Molecular Docking Studies. Four B form DNA decamer sequences, viz. S1 to S4 (Table 1), were used to study the binding of R123. These decamers were formed by 10 base pairs with four specific in the central core. PDB format were used to generate the structural coordinate of these bases.[23]

Table 1. List of Four DNA Decamer Sequences Used for Docking Study

Sl. no.	DNA	sequence
1	S1	5′-d(GATGGCCATC)$_2$
2	S2	5′-d(GATCCGGATC)$_2$
3	S3	5′-d(GGCAATTGCC)$_2$
4	S4	5′-d(GGCTTAAGCC)$_2$

Autodock-Vina program (version 1.1.2) from The Scripps Research Institute[24] and MOE program from CCG Canada were used to study the docking calculation. A three-dimensional grid box of 24 × 26 × 30 with grid spacing of 1.0 Å centered at coordinate x = −3.002, y = 0.008, z = 15.212 were used to cover the full length of DNA, so that the dye molecule can explore all the possible binding sites in each DNA sequence during the docking study.[25−27] Twenty different poses were requested within the energy range of 2 kcal/mol for each docking calculation. A distance criterion of 3 Å was kept fixed for the analysis of hydrogen bonding during docking.

Docking calculations using the MOE program were conducted using Alpha PMI as the placement methodology. The docked poses obtained thus were further refined using the force field method available in the MOE program. The docking was done by placing the R123 molecule in the minor groove of DNA, and the search space was set to the pocket. This enabled the MOE program to search the binding poses in the minor groove only. Once the R123 was placed, the docking run was initiated with the input parameters described above.

Solvent accessible surface area (SASA) of the drug molecule in the receptor bound state provides useful information about the binding characteristics of the drug molecule. SASA analysis was performed using the MOE program. The SASA value of free R123, free DNA, and the R123−DNA complex were determined, and these values were used to determine the hydrophobic contribution of free energy of binding and heat capacity change of binding. The conformations of lowest RMSD (root-mean-square deviation)[28] values were taken in each case to determine the SASA values.

Absorbance Spectral Studies. A Shimadzu Pharmaspec UV-1700 spectrophotometer connected with a PC (Shimadzu Corporation, Tokyo, Japan) equipped with a thermoelectrically controlled cell holder (model TCC 240A) under stirring at 25 ± 0.1 °C in quartz cells of the 1.00 cm path length was used to measure the absorbance spectra.

Fluorescence Spectral Studies. A Hitachi spectrofluorimeter (Hitachi Corporation, Tokyo, Japan) equipped with a thermoelectrically controlled cell holder in matched quartz cells of 1.00 cm path length under stirring at 25 ± 0.5 °C was used to measure fluorescence spectra.

Determination of Affinity Constants. The binding of Rhodamine 123 with CT DNA were evaluated by Benesi Hildebrand plot, noncooperative Scatchard analysis, cooperative Scatchard analysis and Hill analysis.[18,29]

Fluorescence Quenching Studies. 10 mM Solution of $K_4[Fe(CN)_6]$ was used to measure the fluorescence quenching study.[30,31]

UV-Optical Melting Study. A Jasco V-630 unit equipped with the Peltier controlled Jasco PAC-743 model accessory (Jasco International Co. Ltd. Tokyo, Japan) was used to study the absorbance of CT-DNA against change of temperature.[31,32]

Circular Dichroic Study. All circular dichroic measurements were performed by a JASCO: J-815 spectropolarimeter (Japan Spectroscopic Ltd., Japan) controlled by a PC. A rectangular quartz cell having 1 cm path length was used for all CD measurements performing at 25 ± 0.5 °C as reported earlier.[32,33]

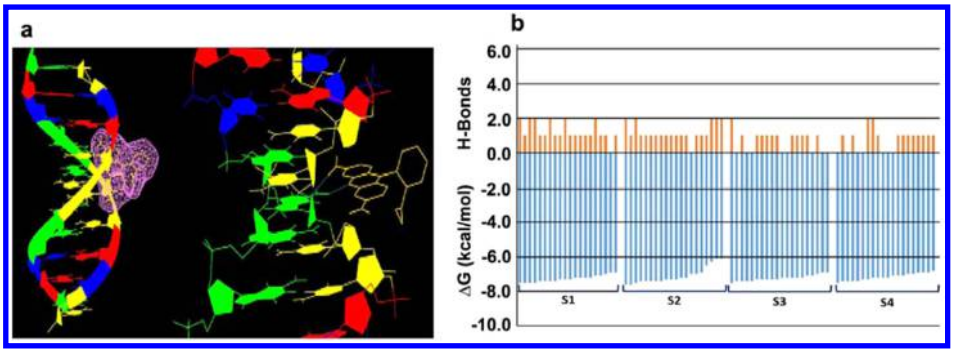

Figure 2. (a) Docking picture of R123 to the minor groove of DNA. (b) Number of hydrogen bond and free-energy values of binding obtained from Autodock-Vina.

dx.doi.org/10.1021/jp509326r | J. Phys. Chem. B XXXX, XXX, XXX−XXX

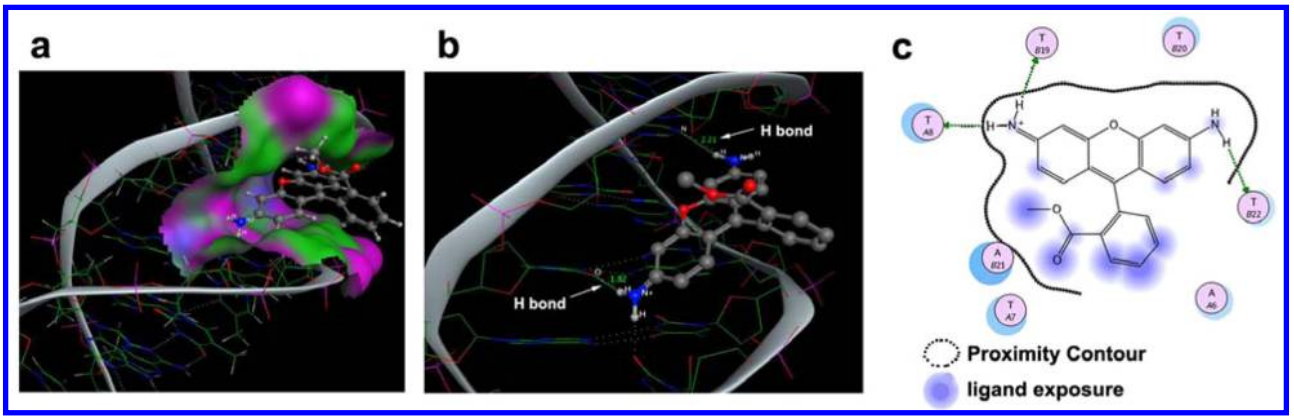

Figure 3. Molecular docking using MOE. (a) R123 pose in the minor groove of DNA. (b) Hydrogen bonds between R123 and DNA bases (indicated with the distances). (c) Two-dimensional interaction diagram of R123−DNA system (buttons with A and T represent adenine and thymine bases in DNA).

Table 2. Table for Different Thermodynamic Properties Obtained from MOE Docking Studies

molecule	SASA (Å^2)	ΔSASA (Å^2)	ΔG_{hyd} (kcal/mol)	ΔC_p (cal/mol K)	binding free energy ΔG (kcal/mol)
R123	581.96039				
S1	4130.7988	−558.33	−12.28 ± 2.79	−153.54 ± 19.19	−7.81
R123-S1 complex	4154.4253				
S2	4131.6802	−519.21	−11.42 ± 2.59	−142.75 ± 17.84	−8.24
R123-S2 complex	4194.4292				
S3	4162.2700	−462.24	−10.17 ± 2.31	−127.12 ± 15.89	−7.37
R123-S3 complex	4281.9858				
S4	4103.6621	−467.16	−10.27 ± 2.33	−128.47 ± 16.06	−8.04
R123-S4 complex	4218.4600				

Isothermal Titration Calorimetric Studies. To study the heat capacity change and enthalpy of binding isothermal titration calorimetric experiments were performed using a VP ITC calorimeter as reported earlier.[32] Aliquots of degassed CT-DNA solution (2.4 mM) were injected from a rotating syringe (1500 rpm) into the isothermal sample chamber containing the R123 solution (5 μM).

■ RESULT AND DISCUSSION

Molecular Docking Studies. Molecular docking study of DNA−Rhodamine 123 interaction clearly indicates that R123 prefers to bind in the minor groove of DNA. This is due to the fact that the banana shape structure of R123 fit to the minor groove of DNA and the narrower and deeper shape of the minor groove offers several points of close contact with R123 via hydrogen bonds, van der Waals forces, etc. (Figure 2a). Binding free energy values obtained from Autodock-Vina program poses of R123 were found to be in the range from −7.6 to −6.1 kcal/mol (Figure 2b and Tables S1−S4 of the Supporting Information).

Eighty docked poses were obtained with four DNA sequences using Autodock-Vina, while 30 poses were obtained using the MOE program. It was clear that the number of intermolecular H-bonds observed in the docked poses obtained with Vina did not exceed two H bonds per docked pose (Figure 2b, upper bar). The total number of docked pose from Autodock-Vina without any H bonding were found to be 17, while single H bonds were present in 49 docked poses and 14 binding poses contained two H bonds. R123 complexes with S1 & S2 contained 24 and 23 H bonds, respectively, while the complexes with S3 & S4 were found to contain 13 and 15 H bonds, respectively (Figure 2b).

The orientation of R123 molecule in the minor groove is such that its carboxy-phenyl ring is orthogonal to the rest of the molecule and is exposed to the outside of the minor groove in contact with solvent environment as previously reported for Rhodamine-B.[18] H-bonds have been observed between terminal NH_2 groups of R123 and DNA bases or sugar residues. Another type of hydrogen bond has also been observed between ring oxygen of R123 and NH atoms of DNA base (e.g., guanine NH_2) (Figure 2). The size of binding site in docked complexes shows that R123 occupies three base pairs of DNA. No evidence of specific binding preference of R123 was obtained from the data set of 80 binding poses in the minor groove of four DNA duplex sequences (S1−S4). All the minor groove poses of R123 were found to be dispersed over the entire length of DNA sequences with almost all possible base pair sets showing no statistically significant binding site preference. Also, the difference in the number of H bonds did not correlate with binding free-energy values, and therefore, no sequence specificity could be established.

On the other hand, docking with MOE program also provided the minor groove binding poses of R123 (Figure 3). MOE program also predicted the free-energy range from about −7.81 to −8.24 kcal/mol (Table 2 and Tables S5−S8 of the Supporting Information). Figure 3 illustrates the position of R123 in the DNA bound form. Several hydrogen bonds were also observed in the docked poses (Figure 3b) as seen in the case with Autodock-Vina docked poses. In addition to this, 2D interaction maps were also generated to illustrate the overall bonding pattern and solvent-exposed surface area of each R123 pose within the DNA minor groove, as shown in Figure 3c.

From docking study, it was observed that R123 deeply penetrates (near about 3 Å from the surface of DNA) to the

dx.doi.org/10.1021/jp509326r | J. Phys. Chem. B XXXX, XXX, XXX−XXX

minor groove and is largely driven by hydrophobic interactions between R123 and DNA minor groove. To measure the hydrophobic free energy of binding (ΔG_{hyd}), the change in solvent accessible surface area (ΔSASA) of R123 and DNA sequences (S1−S4) were determined (Table 2) during complex formation and observed that the values were in the range of −462.24 to −558.33 Å^2. The corresponding values of ΔG_{hyd} were determined using the equation $\Delta G_{hyd} = (22 \pm 5)$ ΔSASA as stated by Record, Jr. and co-worker.[34] The heat capacity change of binding were also determined using the equation $\Delta G_{hyd} = (80 \pm 10)\ \Delta C_{p.}$[35] From our experiment, we observed that the values of ΔG_{hyd} were in the range from −10.17 to −12.28 kcal mol^{-1} and values of ΔC_p were in the range from −127.12 to −153.54 cal mol^{-1}K^{-1} for binding of R123 to S1−S4. These values were further measured by the UV melting process and isothermal calorimetry ITC (vide infra), and all experiments indicate a large hydrophobic contribution during the binding process.

Spectroscopic Results. The absorbance spectra of R123 (1.8 μM) are presented in Figure 4a with increasing

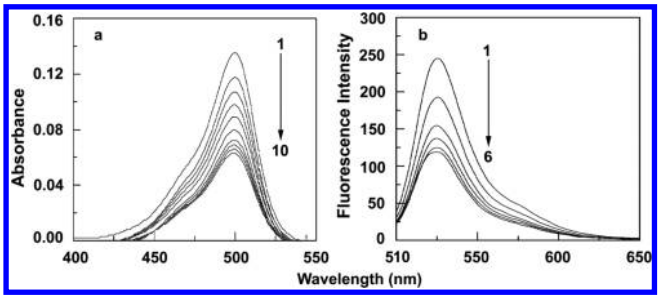

Figure 4. (a) Absorbance spectra of R123 (1.8 μM) in the presence of 0, 8.5, 17.0, 25.5, 34.0, 42.5, 51.0, 59.5, 68.0, 76.5 μM of DNA (1 to 10). (b) Fluorescence spectra of R123 (1.0 μM) in the presence of 0, 9, 18, 27, 36, 45 μM of DNA (1 to 6).

concentration of CT-DNA. A little blue shift (near about 2 nm) and hypochromic effect was observed due to the binding of R123 to DNA. However, lack of any clear isosbestic point may be indicative of more than one type of binding, or a 1:1 R123:DNA stoichiometry could not be characterized during interaction.[36]

R123 showed florescence spectra in the range of 510−650 nm when excited at 506 nm. With increasing concentration of DNA, the fluorescence intensity of R123 decreased due to complex formation (Figure 4b). A very little red shift of maximum wavelength also indicates the complex formation. The optical properties of free and bound dye are presented in Table 3.

Table 3. Summary of Optical Properties of Free and Bound R123[a]

absorbance	λ_{max} (free)	500 nm
	λ_{max} (bound)	498 nm
	ε_f (at λ_{max})	75000 M^{-1} cm^{-1}
	ε_b (at λ_{max})	35000 M^{-1} cm^{-1}
fluorescence	λ_{max} (excitation)	506 nm
	λ_{max} (emission)	525 nm
	F_b/F_0	0.48

[a]Average of three data. Optical properties were determined in CP buffer containing 5 mM Na_2HPO_4, pH 7.0, at 25.0 °C.

Evaluation of Binding Parameters. The data obtained from spectrophotometric and fluorimetric titrations were analyzed by various methods to obtain different binding parameters (Figure 5). The binding analyses revealed that

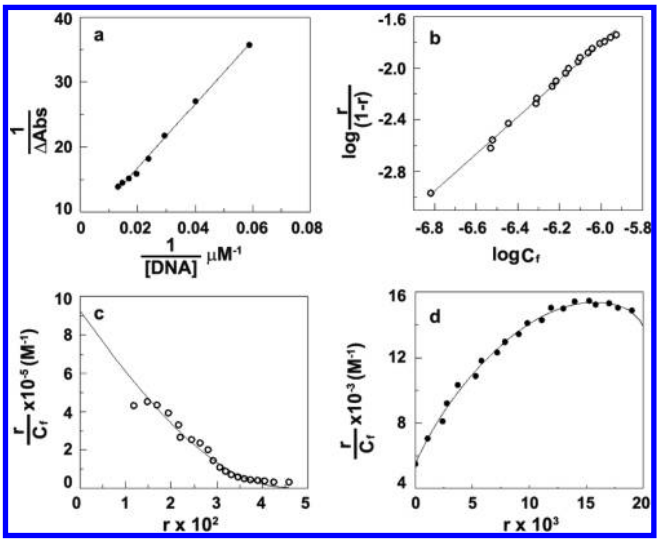

Figure 5. Evaluation of binding parameters by (a) Benesi Hildebrand analysis, (b) Hill analysis, (c) noncooperative Scatchard analysis, and (d) cooperative Scatchard analysis.

binding constant of the rhodamine 123−DNA complex were in the range of 10^5 M^{-1} in both cases. Noncooperative Scatchard analysis of spectrophotometric and fluorimetric data showed that the binding constants were 9.69×10^5 and 7.60×10^5 M^{-1}, where as the number of excluded binding sites were 9.3 base pair and 12.2 base pair, respectively (Table 4). These results are in good agreement with that of the docking study. The Hill analysis and cooperative Scatchard analysis showed that binding was cooperative in nature at very low concentration of dye and gradually became noncooperative at higher dye concentration. The value of $K \times \omega$ obtained from cooperative Scatchard analysis is in the similar range to the binding constant obtained from noncooperative analysis as found earlier.[32,33] All the data obtained from spectrophotometric and fluorimetric studies are listed in Table 4.

Ionic Strength Dependence of the Binding and Parsing of the Free Energy of Binding. To study the effect of salt concentration on the overall binding process, the binding studies were performed at three different salt concentrations of [Na^+], 10, 20, and 50 mM, using spectrophotometric titration. Binding constants at each salt concentration were evaluated using noncooperative Scatchard analysis.

It was observed that overall binding constant decreases moderately at high salt concentration. The following relationship between K and sodium ion concentration (eq 1) has been derived previously.[29,30]

$$\frac{\delta \log K}{\delta \log[Na^+]} = -Z\Psi \qquad (1)$$

where Z is the apparent charge on the bound ligand and ψ is the fraction of the [Na^+] bound per DNA phosphate. Plot of log K versus log [Na^+] yielded a straight line showing a decrease in the binding constant with increasing salt concentration (Figure 6a).

dx.doi.org/10.1021/jp509326r | J. Phys. Chem. B XXXX, XXX, XXX−XXX

Table 4. Binding Data Obtained from Spectrophotometric and Fluorimetric Study[a]

experimental method	method of analysis	binding constant K (M^{-1})	n	ω	$K \times \omega$ (M^{-1})
spectrophotometric	Benesi–Hildebrand	0.142×10^5	–	–	
	noncooperative scatchard	9.69×10^5	9.3	–	
	cooperative scatchard plot	5.51×10^3	19.2	180.91	9.97×10^5
	Hill plot	906.8	–	1.43	1296
fluorimetric	Benesi–Hildebrand	1.15×10^4	–	–	
	noncooperative scatchard	7.60×10^5	12.2	–	
	cooperative Scatchard plot	4.78×10^3	20.1	176.52	8.44×10^5
	Hill plot	869.6	–	1.52	1321

[a]Average of four determinations. Binding constants (K) and the number of occluded sites (n) refer to solution conditions of CP buffer containing 5 mM Na_2HPO_4, pH 7.0 at 25 °C. ω is the cooperativity factor.

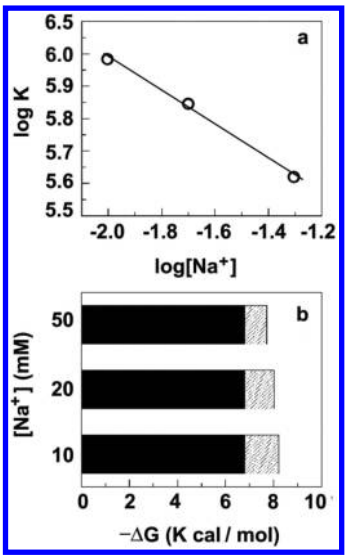

Figure 6. (a) log K vs log[Na^+] plot. (b) The solid parts and hatched parts indicate the nonpolyelectrolytic (ΔG_t) and the polyelectrolytic (ΔG_{pe}) contribution, respectively, to the binding free energy. In all cases, the values of K were obtained from noncooperative Scatchard analysis.

The slope $Z\Psi$ (−0.52) indicates the number of ions released during binding. A similar value of slope were also observed for monocationic molecules binding to double-stranded DNAs and RNAs.[22,31] The observed free energy can be divided into two contributions, the nonpolyelectrolytic contribution (ΔG_t) and the polyelectrolytic contribution (ΔG_{pe})[37,38] using the following equation:

$$\Delta G = -RT \ln K = \Delta G_t + \Delta G_{pe} \quad (2)$$

Record and co-workers[39] have shown that $\Delta G_{pe} = -(Z\Psi)RT \ln[MX]$, where MX is the monovalent salt concentration. ΔG_{pe} is the free-energy contribution due to release of condensed counterions from DNA on binding of the dye. We observed that ΔG_{pe} is smaller ΔG_t in magnitude and value of ΔG_t remained invariant at all ionic strengths, while the ΔG_{pe} contribution decreased with increasing concentration of [Na^+] ion (Table 5 and Figure 6b), indicating that the binding process was forced by both electrostatic (high) and non-electrostatic contribution (low).

Fluorescence Quenching Studies. To study the mode of binding of R123 to DNA, the quenching of fluorescence intensity of the R123–DNA complex were observed in the presence of $[Fe(CN)_6]^{4-}$ (Figure 7). If the small molecule is buried within the DNA helix by intercalation, very little or no change in fluorescence intensity is expected, as anionic quencher is not able to penetrate within the negatively charged DNA helix. From our experiment, we observed that the quenching constants for free and bound R123 were 123 M^{-1} and 72 M^{-1}, respectively. This clearly indicates that R123 does not intercalate into the DNA and remains open to $[Fe(CN)_6]^{4-}$ after binding (groove binding mode). This result is highly significant with docking studies.

Table 5. Binding Constants at Different Salt Concentration Determined by Spectrophotometric Process and Analyzed by Scatchard Analysis[a]

salt concentration (mM)	binding constant $K \times 10^{-5}$ (M^{-1})	ΔG_t (cal/mol)	ΔG_{pe} (cal/mol)	ΔG_{obs} (cal/mol)
10	9.69	−6788	−1427	−8215
20	7.04	−6814	−1212	−8026
50	4.21	−6791	−928	−7719

[a]Average of four determinations. Binding constants (K) were determined in CP buffer containing 5, 10, and 25 mM Na_2HPO_4, pH 7.0, at 25.0 °C.

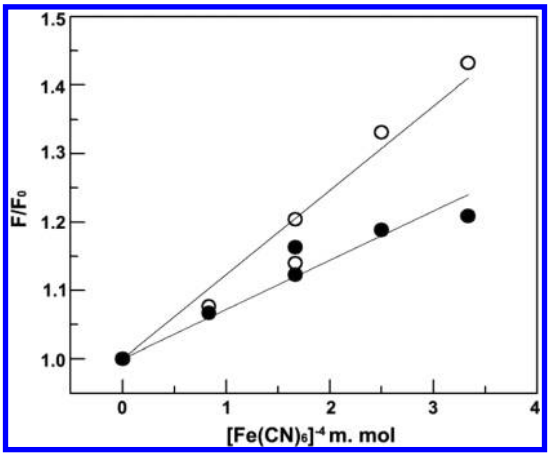

Figure 7. Quenching of florescence intensity of free (o) and bound (●) R123 with increasing concentration of $[Fe(CN)_6]^{4-}$.

Determination of Binding Parameters Using UV Optical Melting Study. UV melting study was used to determine the various thermodynamic and binding parameters like Van't Hoff enthalpy, molar specific heat change, enthalpy of binding, calorimetric enthalpy, and binding constant.

Determination of Van't Hoff Enthalpy. The Van't Hoff enthalpy, ΔH_V, was calculated using the equation as our earlier paper[31]

dx.doi.org/10.1021/jp509326r | J. Phys. Chem. B XXXX, XXX, XXX–XXX

$$\Delta H_V = (2 + 2n)RT_m^2(\delta\alpha/\delta T)_{T=T_m} \quad (3)$$

where α is the fraction of single strands in the duplex state, R is the universal gas constant, T_m is the melting temperature, and n is the number of strand. From the melting curve (Figure 8a), it

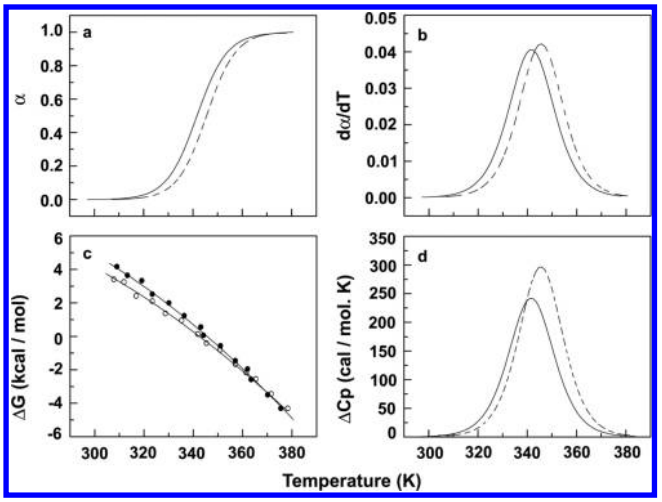

Figure 8. Plot indicating (a) fraction of denaturation vs temperature for free DNA (solid line) and DNA−R123 complex (broken line). (b) Derivative of fraction of denaturation vs temperature for DNA (solid line) and DNA−R123 complex (broken line). (c) Gibbs free energy of melting of DNA (solid line) and DNA-R123 complex (broken line) vs temperature. (d) Heat capacity change during the melting of DNA (solid line) and DNA−R123 complex (broken line) vs temperature.

was obtained that the melting point of free and bound DNA were 341.7 and 346.8 K, where the Van't Hoff enthalpies were 5.6 and 6.02 kcal/mol, respectively, which was similar to that determined by DSC[40] (Table 6). The melting data indicates that the DNA helix stabilize moderately on binding of R123, which was also observed in the case of other molecules binding to DNA and RNA.[30−32,42]

Determination of Molar Heat Capacity Change and Enthalpy of Binding. In previous equation (eq 3), during the determination of Van't Hoff enthalpy, it was assumed that enthalpy change is independent of temperature. From our knowledge, we know that enthalpy is dependent on temperature, and according to Kirchhoff's equation

$$\delta\Delta H/\delta T = \Delta C_p \quad (4)$$

where ΔH is enthalpy change, T is temperature, and ΔC_p is the molar heat capacity change. We fit the Gibbs free energy of melting according to the following equation as stated by Bruylants et al.[41]

$$\Delta G(T) = \Delta H_m(1 - T/T_m) + \Delta C_p[(T - T_m) - T \ln(T/T_m)] \quad (5)$$

where $\Delta G(T)$ is the Gibbs free energy change at temperature T, ΔH_m is the enthalpy change at melting temperature, T_m is the melting temperature, and ΔC_p is the molar heat capacity change. Plotting the values of $\Delta G(T)$ against T and fitting by eq 5 (Figure 8c), we obtained the values of T_m, ΔH_m, and ΔC_p of free and bound DNA (see Figure 8). The ΔH_m were 40266 and 47017 cal/mol, T_m were 341.7 and 346.8 K, and ΔC_p were 241 cal/mol K and 295 cal/mol K for free and bound DNA, respectively (Table 6).

We used these data again to determine the enthalpy change and heat capacity change of binding. The enthalpy change at temperature T can be calculated according to Kirchhoff's law by following equation

$$\Delta H(T) = \Delta H_m + \Delta C_p(T - T_m) \quad (6)$$

From this equation, we obtained 29734 and 32711 cal/mol for the enthalpy change (ΔH) for free and bound DNA at 25 °C, respectively.

The enthalpy of binding and molar heat capacity change of binding were obtained by the following

$$\text{dsDNA} \rightarrow \text{ssDNA} + \Delta H_{free} \quad (7)$$

$$\text{dsDNAR123} \rightarrow \text{ssDNA} + \text{R123} + \Delta H_{bound} \quad (8)$$

Subtracting eq 8 from 7, we obtained

$$\text{dsDNA} + \text{R123} \rightarrow \text{dsDNAR123} + (\Delta H_{free} - \Delta H_{bound}) \quad (9)$$

Using the above equations, we obtained an enthalpy of binding of R123 to DNA of −2977 cal/mol at 25.0 °C. From this experiment, it is clear that the binding was favored by negative enthalpy change and positive entropy change (Table 6).

Determination of Calorimetric Enthalpy. The calorimetric enthalpy of melting varies several times from Van't Hoff

Table 6. Binding Data Obtained from Optical Melting Studies

	free DNA	bound DNA
melting temperature (K)	341.7	346.8
Van't Hoff enthalpy ΔH_V (cal/mol) from fraction of binding	56011	60197
Van't Hoff enthalpy ΔH_V by plotting $-R \ln K$ vs $1/T$ (cal/mol)	41740	46650
enthalpy change at melting point ΔH_m (cal/mol)	40266	47017
heat capacity change ΔC_p (cal/mol K)	241	295
enthalpy change at 25.0 °C ΔH (cal/mol)	29734	32711
calorimetric enthalpy (cal/mol)	6330	7748
binding affinity at melting point K_m (M^{-1})		2.55×10^5
binding affinity at 25.0 °C (M^{-1})		5.08×10^5
enthalpy of binding at 25.0 °C (cal/mol)		29734−32711 = −2977
entropy of binding at 25.0 °C (cal/mol K)		16.29
heat capacity change during complex formation ΔC_p (cal/mol K)		(241−295)/0.4 = −135
$\Delta G_{hydro} = 80 \times \Delta C_p$ (kcal/mol)		−10.8
$\Delta H_v/\Delta H_{cal}$	8.40	9.69

dx.doi.org/10.1021/jp509326r | J. Phys. Chem. B XXXX, XXX, XXX−XXX

enthalpy due to various factors,[42] like intra- and intermolecular hydrogen bonding, folding, stacking between bases, etc. So the determination of calorimetric enthalpy is highly necessary for details study of binding phenomena. Several groups used a differential scanning calorimeter (DSC) to determine calorimetric enthalpy of several nucleic acids like DNA[40−42] and RNA.[31,32] Many times the DSC cannot be used due to several factors like unavailability, high sample concentration, baseline problems, etc. though the melting profile of optical melting and DSC are the same.[31,32]

In this paper, we used a different method to determine the calorimetric enthalpy. It was concluded that the heat consumed by DNA was totally used to unwind the DNA helix. As a result, the heat change is proportional to the unwinding of the DNA helix, and we can write

$$\Delta \mathrm{H} \propto \alpha$$

$$\text{that is, } \Delta H = m\alpha \tag{10}$$

where ΔH is enthalpy change for melting, α is the fraction of denatured DNA, and m is the proportionality constant.

$$\Delta C_p = \delta \Delta \mathrm{H}/\delta \mathrm{T} = \delta(m\alpha)/\delta \mathrm{T} = m\delta\alpha/\delta \mathrm{T} \tag{11}$$

Or $\Delta C_p{}^{\mathrm{m}} = m\ (\delta\alpha/\delta T)_{T=T_m}$ where $\Delta C_p{}^{\mathrm{m}}$ is the molar heat capacity at the melting point, which is assumed to be the same as ΔC_p (241 cal/mol K for free DNA and 295 cal/mol K for bound DNA).

So the calorimetric enthalpy is the area under the curve and mathematically can be written as

$$\Delta H_{\mathrm{cal}} = \int_{T_1}^{T_2} \Delta C_p{}^{\mathrm{m}}\, \mathrm{d}T \tag{12}$$

where T_1 and T_2 are the temperature of fully natured and fully denatured DNA structure. From this above equation we obtained the calorimetric enthalpy of free and bound DNA melting were 6330 and 7748 cal/mol, respectively, which were similar to that obtained from the DSC experiment by other groups.[40,41] From our experiment, we observed that ΔH_{v} is higher than ΔH_{cal} in both free and bound DNA. The ratio of $\Delta H_{\mathrm{v}}/\Delta H_{\mathrm{cal}}$ provides a powerful test for the model of DNA denaturation and gives the energy per mol of the cooperative unit in the equilibrium, while ΔH_{cal} gives the energy per mol of DNA. Here the ratio of $\Delta H_{\mathrm{v}}/\Delta H_{\mathrm{cal}}$ of 8.40 and 9.69, respectively, for free and bound DNA indicates that the melting process is not fully cooperative and lots of stacking, hydrogen bonding, etc. were present, which were also predicted by docking studies. The calorimetric enthalpy change and $\Delta C_p{}^{\mathrm{m}}$ were also used to determine the enthalpy of binding and heat capacity change of the binding process, as stated by Waring and co-workers.[43] They divided the difference of calorimetric enthalpies of free and bound DNA by a binding ratio (r value) to determine binding enthalpy. In our case, the difference of calorimetric enthalpies and differences of $\Delta C_p{}^{\mathrm{m}}$ values between free and bound. DNA were −1.42 kcal/mol and −54 cal/mol K, respectively, at melting temperature. The binding ratio of dye/DNA taken for this experiment (highest ratio of dye/DNA during optical melting experiment) was 0.4. From these data, we observed that the enthalpy change for the R123−DNA binding process was −3.54 kcal/mol and heat capacity change ΔC_p was −135 cal/mol K, respectively. Both these values are in good agreement with that obtained from docking (Table 2) and other experiments like ITC (vide infra).

Determination of Binding Constant from UV Melting Study. The melting temperatures of free and bound DNA were used to calculate the binding constant of R123 to DNA using the equation derived by Crothers.[44] From this experiment, we obtained binding constants of the dye−DNA complex of 2.55×10^5 and 5.08×10^5 M^{-1} at melting temperature and 25.0 °C (Table 6), respectively. These results are in reasonable agreement with the values obtained from other binding studies.

Conformational Aspects of Binding. To study the conformational change of DNA helix, intrinsic CD spectra of CT-DNA in the presence and absence of dye were taken. A large positive band at 275 nm and a large negative band at 245 nm in intrinsic CD spectrum suggest the existence of B-form conformation of CT-DNA. The negative band at 245 nm is due to the helical structure of DNA, and the positive band at 275 nm is due to the stacking interactions between the bases. In the presence of rhodamine 123, the ellipticity of the long wavelength positive band (275 nm) does not change remarkably; however, a little change in the ellipticity of the negative band (245 nm) was observed as the interaction progressed (Figure 9). These phenomena indicate decrease in base-pair helicity; however, perturbations on the helicity and especially base-stacking bands were not as pronounced as being indicative of a transition in DNA conformation. This evidence supports that R123 binds to the groove of DNA. Similar types of results were also observed during the interaction of other minor groove binders and rhodamine B to DNA.[18,45,46]

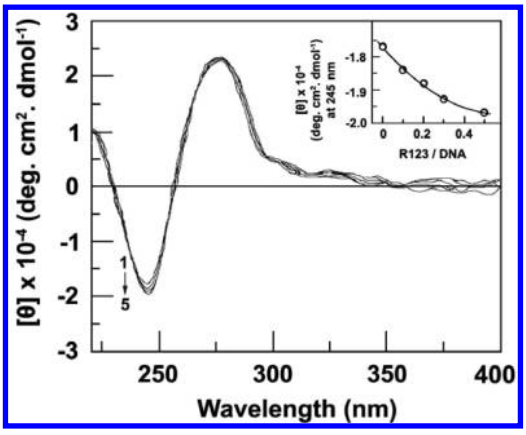

Figure 9. Intrinsic CD spectra of CT DNA (60 μM) in the presence of 0, 6, 12, 18, and 30 μM of R123 (spectra 1 to 5). Inset: θ vs R123/DNA ratio at 245 nm.

Isothermal Titration Calorimetric Studies. Isothermal titration calorimetry (ITC) (Figure 10) is an effective tool to study the thermodynamic parameters such as Gibbs free-energy change (ΔG), enthalpy change (ΔH), entropy change (ΔS), number of binding sites (N), and the binding constant (K).

Each point in the lower panel of Figure 10 indicates that the heat change due to single injection of the respective DNA into R123. Each point was corrected by corresponding dilution heats derived from the titration of identical amounts of DNA into the buffer alone. These data were fitted to a single site binding curve. From the fitted data, we obtained an association constant (K) of $(1.21 \pm 0.70) \times 10^5$ M^{-1}, an enthalpy change (ΔH) of −3.41 kcal/mol, an entropy change (ΔS) of 11.96 cal/mol K, and a binding site size ($1/N$) of 7.8 base pairs. Enthalpy reflects heat differences between reactants (free DNA, free R123) and products (DNA−R123 complex) due to the net

dx.doi.org/10.1021/jp509326r | J. Phys. Chem. B XXXX, XXX, XXX−XXX

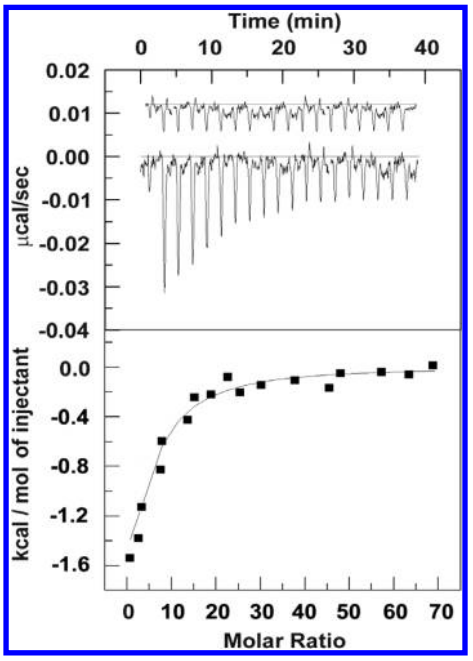

Figure 10. Representative ITC profile for the titration of CT DNA into a solution of Rhodamine 123. The top panel represents the heat burst curves due to successive injection of DNA solution into the Rhodamine 123. The bottom panel represents the corresponding normalized heat signals versus molar ratio of DNA. The control heat bursts of titration of the dye into buffer are presented in the top panel (curves offset of clarity).

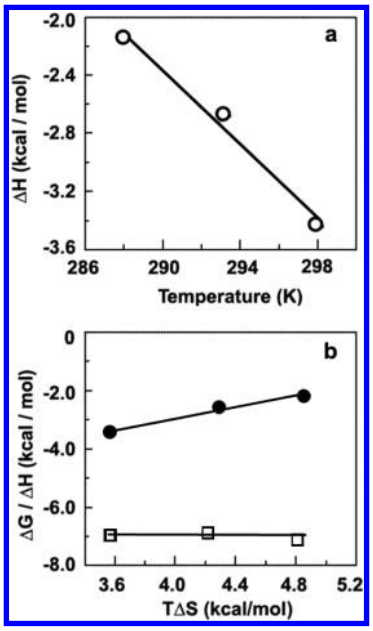

Figure 11. (a) Change of enthalpy of binding of R123 and DNA vs temperature. (b) Enthalpy entropy compensation plot. (● indicates the enthalpy and □ indicates the free-energy change.)

bond formation or breakage. The negative value of enthalpy indicates a net release of heat energy as the products are at a lower energy level than the reactants. On the other hand, entropy reveals the ease of distribution of binding energy among molecular energy levels. The positive value of entropy is associated with an increase in disorder and vice versa. The release of structured water molecules surrounding the binding surfaces of DNA is commonly considered to be a source of positive entropy as a result of an increase in the disorder of the system but depends on the precise balance of solvent interactions with the free binding partners and within the binding complex.

The binding affinity values evaluated from the ITC data are comparable with thermodynamic parameters obtained from other methods like spectroscopy and optical melting (vide supra).

Heat Capacity Change. The heat capacity changes (ΔC_p) of any reaction can be determined from the temperature dependence of enthalpy change (eq 4) during the reaction. A large ΔC_p value is usually indicative of a large hydrophobic effect during the binding process.

Figure11a graphically presents the effect of temperature variation on the ΔH values (see Table 7). The data points were fitted by linear regression, and from the slopes it was observed that ΔC_p for the binding of R123 to DNA was of −127.2 cal/mol K, which is similar to that observed from docking studies and optical melting study. Due to the presence of aromatic ring system in intercalators and groove binder molecules, a large hydrophobic contribution to the binding free energy is expected for their interaction.

From Records relationship,[39] $\Delta G_{hyd} = (80 \pm 10)\Delta C_p$, the hydrophobic free energy was calculated and found to be −10.18 ± 1.27 kcal/mol, which was in good agreement with that obtained from optical melting and docking studies. A slightly negative ΔC_p value that we found here appears to be associated with a minimal sequence specific binding.[47]

Solvent reorganization during the binding process can be studied by enthalpy−entropy compensation.[48,49] The value of slope of ΔH versus $T\Delta S$ unity is an indication of complete compensation. Figure 11b shows the variation of ΔH as a function of $T\Delta S$ with slope 0.99, suggesting almost complete compensation during the binding study.

The observed free energy of dye DNA interaction may be divided into the following contributions.[50,51]

$$\Delta G_{obs} = \Delta G_{conf} + \Delta G_{t+r} + \Delta G_{hyd} + \Delta G_{pe} + \Delta G_{mol}$$

where ΔG_{obs} is the observed binding free energy, calculated from binding constant (K) by the standard Gibbs equation. ΔG_{conf} is the free-energy contribution due to the conformational changes in the DNA helix upon complex formation, ΔG_{t+r} is the free-energy contribution resulting due to the losses of translational and rotational freedom during DNA−dye complex formation, ΔG_{hyd} is the free energy for the hydrophobic transfer of dye from solution to the DNA binding sites, ΔG_{pe} is the electrostatic free energy contribution, ΔG_{mol} is the free-energy contribution for the formation of weak noncovalent bonds, including hydrogen bonds, van der Waals interactions, and other weak forces. For the R123−DNA interaction, ΔG_{obs} was −8.21 kcal/mol. According to Portugal and co-worker,[52] the contribution from conformational changes ΔG_{conf} upon formation of groove binding is near zero. Our docking experiment showed that the conformational free-energy change ΔG_{conf} of DNA during the formation of the R123−DNA complex was in the range of 0.78 to 0.91 kcal/mol for four DNA sequences (S1−S4). To validate our data, we calculated the conformational free energy using intrinsic CD spectra and the free energy value 0.97 kcal/mol thus obtained matches well with that found from the docking study (see the Supporting Information). The free energy associated with loss of translational and rotational freedom was taken as 15 kcal/

dx.doi.org/10.1021/jp509326r | J. Phys. Chem. B XXXX, XXX, XXX−XXX

Table 7. Temperature-Dependent Binding Data Obtained from ITC Experiments[a]

temperature	$K \times 10^{-5}$ (M^{-1})	ΔG (cal/mol)	ΔH (cal/mol)	$T\Delta S$ (cal/mol)	ΔC_p (cal/mol K)	ΔG_{hyd} (kcal/mol)
288	1.85	−6985	−2138	4847	−127.2	−10.18 ± 1.27
293	1.49	−6981	−2690	4291		
298	1.21	−6975	−3410	3565		

[a]All the data in this table are derived from the ITC experiments. Gibbs energy ΔG change and the entropy contribution $T\Delta S$ were determined using the equations $\Delta G = -RT \ln K$, and $T\Delta S = \Delta H - \Delta G$, where T is the temperature, K the binding constant, and ΔH the enthalpy change. ΔG_{hyd} denotes the Gibbs energy contribution from the hydrophobic transfer of binding of the analogs and ΔC_p denotes the heat capacity changes.

mol.[43] These positive free-energy contributions must be less than that of favorable negative contributions driven by a hydrophobic contribution ($\Delta G_{hyd} = -10.18 \pm 1.27$ kcal/mol) and ionic contribution ($\Delta G_{pe} = -1.42$ kcal/mol). After adding the five free-energy contributions (Figure 12), the observed free-energy change was found by

$$\begin{aligned}\Delta G_{obs} &= \Delta G_{conf} + \Delta G_{t+r} + \Delta G_{hyd} + \Delta G_{pe} + \Delta G_{mol} \\ &= 0.97 + 15 + (-10.18) + (-1.42) + \Delta G_{mol} \\ &= 4.37 + \Delta G_{mol}\end{aligned}$$

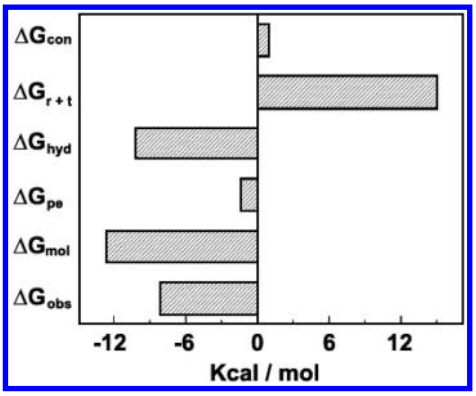

Figure 12. Different types of free-energy contributions for the R123−DNA interaction.

From our experiment we found that $\Delta G_{obs} = -8.21$ kcal/mol. Using this value, we obtained $\Delta G_{mol} = -12.58$ kcal/mol. This value indicates that forces associated with direct contacts between R123 and DNA plays a significant role during complex formation. The negative favorable energetic contributions ΔG_{mol} and ΔG_{hyd} combined with a minor polyelectrolyte contribution ΔG_{pe} drive the formation of the R123−DNA complex, overcoming the unfavorable free energy due the reduction of translational and rotational freedom and conformational change of DNA helix.

CONCLUSIONS

The computational and biophysical studies of binding of R123 to DNA suggest that R123 binds to DNA quite strongly. The docking study showed that hydrogen bonding and hydrophobic free energy (determined by solvent accessible surface area) contributions play a significant role to stabilize the complex. The remarkable hypochromicity in fluorescence also concludes that the binding of R123 to CT DNA is quite strong. The salt dependence of the DNA binding of R123 indicates that the charge release when DNA interacts with R123 in accordance with the polyelectrolyte theory is −0.52. Thus, the binding constant of the R123−DNA complex was favored by both electrostatic and nonelectrostatic processes. At low concentration of salt (0.01 mol L^{-1}), binding is favored by electrostatic interaction. On the other hand, at a high salt concentration, it is favored by nonelectrostatic processes.

Ferrocyanide quenching study, docking study, and CD spectral analysis suggest that R123 does not intercalate into the DNA helix. Thermal denaturation study suggests that the DNA helix stabilizes due to binding of R123, and the melting point of DNA increases by approximately 5.0 °C. The small change of melting point is also an indication of the nonintercalation mode. A significant difference between Van't Hoff enthalpy and calorimetric enthalpy indicates that the melting process is noncooperative in nature and that there is a lot of stacking present in the DNA helix in both free and bound conditions. The increase of both Van't Hoff and calorimetric enthalpy due to binding of R123 indicates that R123 exothermally binds to DNA, which is further supported by thermodynamic analysis. Since, entropy increases during the binding process, it may be concluded that the binding of R123 to DNA is favored by both negative enthalpy and positive entropy changes. Different types of free energy that contribute to the observed free-energy change suggest that the binding free energy is favored by negative molecular free energy, hydrophobic free energy, and electrostatic free energy, which compensate the positive free energy due to the restriction of rotational and transitional movement and conformational change of DNA. Although, it was assumed that the large negative hydrophobic free energy is the characteristic of intercalators, Chaires[50] and Shaikh[53] showed that groove binders can also have large negative hydrophobic free-energy change during interaction with DNA. Our experiments also support this. From the docking study, it was observed that few parts of the phenyl ring of R123 is exposed to the solvent but maximum part penetrates to the minor groove of DNA (Figure S5 of the Supporting Information), causing a significant change in hydrophobic free energy which supports our experimental observations. We believe that the mode, mechanism, and energetics of binding acquired from our study will help to increase the knowledge on bioactivity of R123.

ASSOCIATED CONTENT

Supporting Information

Detail of docking tables done by Autodock-Vina and MOE. LigX pictures of S1, S2, S3, and S4 with R123 complex. Determination of conformational free-energy change of DNA helix during the binding process. This material is available free of charge via the Internet at http://pubs.acs.org.

AUTHOR INFORMATION

Corresponding Author

*E-mail: maidulaliah@gmail.com or maidul.chem@aliah.ac.in. Tel: +91-33-27062271. Fax: +91-33-40062533.

dx.doi.org/10.1021/jp509326r | J. Phys. Chem. B XXXX, XXX, XXX−XXX

Present Address

[‖]Division of Forensic Science, School of Basic and Applied Sciences, Galgotias University, Plot No.2, Sector 17-A, Greater Noida, Gautam Buddh Nagar, Uttar Pradesh, India.

Notes

The authors declare no competing financial interest.

■ ACKNOWLEDGMENTS

The authors would like to thank Prof. Dipak Dasgupta, Ms. Saptaparni Ghosh, and Ms. Shreyasi Dutta of Saha Institute of Nuclear Physics, Kolkata. The authors also acknowledge the valuable support of Dr. Kakali Bhadra, Ms. Sarita Sarkar of Kalyani University, Prof. Parimal Karmakar, Mr. Dipranjan Laha, and Ms. Sahanaz Khatun of Jadavpur University. P.P. is thankful to UGC for the award of Dr. D.S. Kothari PDF (Grant F.4-2/2006(BSR)/13-557/2011). The award of a Senior Research Fellowship to M.C. by the Council of Scientific and Industrial Research, New Delhi (Grant 09/096(0601)/2009), is acknowledged. M.M.I. wishes to thank Dr. Abhijit Saha, Scientist F, Radiation Chemistry, UGC DAE, Kolkata centre, and Mr. Asif Hasan, Department of English, Aliah University. S.M. thankfully acknowledges partial financial help from the UPE II fund of Jadavpur University sanctioned by University Grants Commission, New Delhi.

■ REFERENCES

(1) Dawson, M. A.; Kouzarides, T. Cancer Epigenetics: From Mechanism to Therapy. *Cell* **2012**, *150*, 12−27.

(2) Pati, H.; Howard, T.; Townes, H.; Lingerfelt, B.; McNulty, L. A.; Lee, M. Unexpected Syntheses of Seco-Cyclopropyltetrahydroquinolines from a Radical 5-Exo-Trig Cyclization Reaction: Analogs of CC-1065 and the Duocarmycins. *Molecules* **2004**, *9*, 125−133.

(3) Sarkar, D.; Das, P.; Basak, S.; Chattopadhyay, N. Binding Interaction of Cationic Phenazinium Dyes with Calf Thymus DNA: A Comparative Study. *J. Phys. Chem. B* **2008**, *112*, 9243−9249.

(4) Li, C. Z.; Liu, Y.; Luong, J. H. T. Impedance Sensing of DNA Binding Drugs Using Gold Substrates Modified with Gold Nanoparticles. *Anal. Chem.* **2005**, *77*, 478−485.

(5) Wanunu, M.; Sutin, J.; Meller, A. DNA Profiling Using Solid-State Nanopores: Detection of DNA-Binding Molecules. *Nano Lett.* **2009**, *9*, 3498−3502.

(6) Cheng, B.; Cai, X. Q.; Miao, Q.; Wang, Z. H.; Hu, M. L. Selective Interactions Between 5-Fluorouracil Prodrug Enantiomers and DNA Investigated with Voltammetry and Molecular Docking Simulation. *Int. J. Electrochem. Sci.* **2014**, *9*, 1597−1607.

(7) Yang, F.; Nickols, N. G.; Li, B. C.; Marinov, G. K.; Said, J. W.; Dervan, P. B. Antitumor Activity of a Pyrrole-Imidazole Polyamide. *Proc. Natl. Acad. Sci. U.S.A.* **2013**, *110*, 1863−1868.

(8) Dervan, P. B. Molecular Recognition of DNA by Small Molecules. *Bioorg. Med. Chem.* **2001**, *9*, 2215−2235.

(9) Emaus, R. K.; Grunwald, R.; Lemasters, J. J. Rhodamine-123 as a Probe of Transmembrane Potential in Isolated Rat-Liver Mitochondria: Spectral and Metabolic Properties. *Biochim. Biophys. Acta* **1986**, *850*, 436−448.

(10) Johnson, L. V.; Walsh, M. L.; Chen, L. B. Localization of Mitochondria in Living Cells with Rhodamne 123. *Proc. Natl. Acad. Sci. U.S.A.* **1980**, *77*, 990−994.

(11) Perriere, N.; Yousif, S.; Cazaubon, S.; Chaverot, N.; Bourasset, F.; Cisternino, S.; Declèves, X.; Hori, S.; Terasaki, T.; Deli, M.; et al. A Functional In Vitro Model of Rat Blood-Brain Barrier for Molecular Analysis of Efflux Transporters. *Brain Res.* **2007**, *1150*, 1−13.

(12) Troutman, M. D.; Thakker, D. R. Rhodamine 123 Requires Carrier-Mediated Influx for its Activity as a P-GlycoProtein Substrate in Caco-2 Cells. *Pharm. Res.* **2003**, *20*, 1192−1199.

(13) Dobson, P. D.; Lanthaler, K.; Oliver, S. G.; Kell, D. B. Implications of the Dominant Role of Transporters in Drug Uptake by Cells. *Curr. Top. Med. Chem.* **2009**, *9*, 163−181.

(14) Biswas, S.; Dodwadkar, N. S.; Sawant, R. R.; Koshkaryev, A.; Torchilin, V. P. Surface Modification of Liposomes with Rhodamine-123-Conjugated Polymer Results in Enhanced Mitochondrial Targeting. *J. Drug Targeting* **2011**, *19*, 552−561.

(15) Gupta, R. S.; Dudani, A. K. Species-Specific Differences in the Toxicity of Rhodamine 123 Towards Cultured Mammalian Cells. *J. Cell Physiol.* **1987**, *130*, 321−327.

(16) Lampidis, T. J.; Bernal, S. D.; Summerhayes, I. C.; Chen, L. B. Selective Toxicity of Rhodamine 123 in Carcinoma Cells In Vitro. *Cancer Res.* **1983**, *43*, 716−720.

(17) Bernal, S. D.; Lampidis, T. J.; Summerhayes, I. C.; Chen, L. B. Rhodamine-123 Selectively Reduces Clonal Growth of Carcinoma Cells in vitro. *Science* **1982**, *218*, 1117−1119.

(18) Islam, M. M.; Chakraborty, M.; Pandya, P.; Masum, A. A.; Gupta, N.; Mukhopadhyay, S. Binding of DNA with Rhodamine B: Spectroscopic and Molecular Modeling Studies. *Dyes Pigm.* **2013**, *99*, 412−422.

(19) Islam, M. M.; Basu, A.; Hossain, M.; Kumar, G. S. Enhanced DNA Binding of 9-ω-Amino Alkyl Ether Analogs of Plant Alkaloid Berberine. *DNA Cell Biol.* **2011**, *30*, 123−133.

(20) Darzynkiewicz, Z.; Traganos, F.; Staiano-Coico, L.; Kapuscinski, J.; Melamed, M. R. Interactions of Rhodamine 123 with Living Cells Studied by Flow Cytometry. *Cancer Res.* **1982**, *42*, 799−806.

(21) Islam, M. M.; Pandey, P.; Kumar, S.; Roy, C. S.; Kumar, G. S. Binding of DNA Binding Alkaloids to tRNA and Comparison to Ethidium through Spectroscopic and Molecular Modeling Studies. *J. Mol. Struct.* **2008**, *891*, 498−507.

(22) Bhadra, K.; Kumar, G. S. Therapeutic Potential of Nucleic Acid-Binding Isoquinoline Alkaloids: Binding Aspects and Implications for Drug Design. *Med. Res. Rev.* **2011**, *31*, 821−862.

(23) Arnott, S.; Campbell-Smith, P. J.; Chandrasekaran, R. Nucleic Acids. In *Handbook of Biochemistry and Molecular Biology*, 3rd ed.; Fasman, G.P., Ed.; CRC Press: Cleveland, 1976; Vol. *II*, pp 411−422.

(24) Trott, O.; Olson, A. Auto Dock Vina: Improving the Speed and Accuracy of Docking with a New Scoring Function, Efficient Optimization, and Multithreading. *J. Comput. Chem.* **2010**, *31*, 455−461.

(25) Seeliger, D.; Groot, B. L. Ligand Docking and Binding Site Analysis with PyMOL and Autodock Vina. *J. Comput.-Aided Mol. Des.* **2010**, *24*, 417−422.

(26) Chang, M. W.; Ayeni, C.; Breuer, S.; Torbett, B. E. Virtual Screening for HIV Protease Inhibitors: A Comparison of Auto Dock 4 and Vina. *PLoS One* **2010**, *5* (e11955), 1−9.

(27) Takatsuka, Y.; Chen, C.; Nikaido, H. Mechanism of Recognition of Compounds of Diverse Structures by the Multidrug Efflux Pump AcrB of Escherichia coli. *Proc. Natl. Acad. Sci. U.S.A.* **2010**, *107*, 6559−6565.

(28) Hevener, K. E.; Zhao, W.; Ball, D. M.; Babaoglu, K.; Qi, J.; White, S. W.; Lee, R. E. Validation of Molecular Docking Programs for Virtual Screening against Dihydropteroate Synthase. *J. Chem. Inf Model.* **2009**, *49*, 444−460.

(29) Islam, M. M.; Kumar, G. S. Small Molecule RNA Interactions: Spectroscopic and Calorimetric Studies on the Binding by the Cytotoxic Protoberberine Alkaloid Coralyne to Single Stranded Polyribonucleotides. *Biochim. Biophys. Acta* **2009**, *1790*, 829−839.

(30) Sarkar, S.; Bhadra, K. Binding of Alkaloid Harmalol to DNA: Photophysical and Calorimetric Approach. *J. Photochem. Photobiol., B* **2014**, *130*, 272−280.

(31) Islam, M. M.; Sinha, R.; Kumar, G. S. RNA Binding Small Molecules: Studies on t-RNA Binding by Cytotoxic Plant Alkaloids Berberine, Palmatine and Comparison to Ethidium. *Biophys. Chem.* **2007**, *125*, 508−520.

(32) Islam, M. M.; Chowdhury, S. R.; Kumar, G. S. Spectroscopic and Calorimetric Studies on the Binding of Alkaloids Berberine, Palmatine and Coralyne to Double-Stranded RNA Polynucleotides. *J. Phys. Chem. B* **2009**, *113*, 1210−1224.

(33) Islam, M. M.; Basu, A.; Kumar, G. S. Binding of 9-ω-Amino Alkyl Ether Analogs of Plant Alkaloid Berberine to Poly(A): Insights into Self-Structure Induction. *Med. Chem. Commun.* **2011**, *2*, 631−637.
(34) Livingstone, J. R.; Spolar, R. S.; Record, M. T., Jr. Contribution to the Thermodynamics of Protein Folding from the Reduction in Water-Accessible Nonpolar Surface Area. *Biochemistry* **1991**, *30*, 4237−4244.
(35) Ha, J. H.; Spolar, R. S.; Record, M. T., Jr. Role of the Hydrophobic Effect in Stability of Site-Specific Protein-DNA Complexes. *J. Mol. Biol.* **1989**, *209*, 801−816.
(36) Rehman, S. U.; Yaseen, Z.; Husain, M. A.; Sarwar, T.; Ishqi, H. M.; Tabish, M. Interaction of 6 Mercaptopurine with Calf Thymus DNA: Deciphering the Binding Mode and Photoinduced DNA Damage. *PLOS One* **2014**, *9*, e93913.
(37) Chaires, J. B.; Satyanarayana, S.; Suh, D.; Fokt, I.; Przewloka, T.; Priebe, W. Parsing the Free Energy of Anthracycline Antibiotic Binding to DNA. *Biochemistry* **1996**, *35*, 2047−2053.
(38) Chaires, J. B. Dissecting the Free Energy of Drug Binding to DNA. *Anti-Cancer Drug Des.* **1996**, *11*, 569−580.
(39) Record, M. T.; Anderson, C. F.; Lohman, T. M. Thermodynamic Analysis of Ion Effects on the Binding and Conformational Equilibria of Proteins and Nucleic Acids: The Roles of Ion Association or Release, Screening, and Ion Effects on Water Activity. *Q. Rev. Biophys.* **1978**, *11*, 103−178.
(40) Duguid, J. G.; Benevides, J. M.; Thomas, G. J., Jr. DNA Melting Investigated by Differential Scanning Calorimetry and Raman Spectroscopy. *Biophys. J.* **1996**, *71*, 3350−3360.
(41) Bruylants, G.; Wouters, J.; Michaux, C. Differential Scanning Calorimetry in Life Science: Thermodynamics, Stability, Molecular Recognition and Application in Drug Design. *Cur. Med. Chem.* **2005**, *12*, 2011−2020.
(42) Kabir, A.; Hossain, M.; Kumar, G. S. Thermodynamics of the DNA Binding of Biogenic Polyamines: Calorimetric and Spectroscopic Investigations. *the Journal of Chemical Thermodynamics* **2013**, *57*, 445−453.
(43) Fenfei Leng, F.; Chaires, J. B.; Waring, M. J. Energetics of Echinomycin Binding to DNA. *Nucleic Acids Res.* **2003**, *31*, 6191−6197.
(44) Crothers, D. M. Statistical Thermodynamics of Nucleic Acid Melting Transitions with Coupled Binding Equilibria. *Biopolymers* **1971**, *10*, 2147−2160.
(45) Nguyen, B.; Hamelberg, D.; Bailly, C.; Colson, P.; Stanek, J.; Brun, R.; Neidle, S.; Wilson, W. D. Characterization of a Novel DNA Minor-Groove Complex. *Biophys. J.* **2004**, *86*, 1028−1041.
(46) Nazif, M. A.; Rubbiani, R.; Alborzinia, H.; Kitanovic, I.; Wolfl, S.; Ott, I.; Sheldrick, W. S. Cytotoxicity and Cellular Impact of Dinuclear Organoiridium DNA Intercalators and Nucleases with Long Rigid Bridging Ligands. *Dalton Trans.* **2012**, *41*, 5587−5598.
(47) Murphy, F. V.; Churchill, M. E. Nonsequence-Specific DNA Recognition: A Structural Perspective. *Structure* **2000**, *15*, R83−89.
(48) Jen-Jacobson, L.; Engler, L. E.; Jacobson, L. A. Structural and Thermodynamic Strategies for Site-Specific DNA Binding Proteins. *Structure* **2000**, *8*, 1015−1023.
(49) Chaires, J. B. A Thermodynamic Signature for Drug-DNA Binding Mode. *Arch. Biochem. Biophys.* **2006**, *453*, 26−31.
(50) Chaires, J. B. Energetic of Drug DNA Interactions. *Biopolymers* **1997**, *44*, 201−215.
(51) Haq, I. Thermodynamics of Drug DNA Interactions. *Arch. Biochem. Biophys.* **2002**, *403*, 1−15.
(52) Barcelo, F.; Capo, D.; Portugal, J. Thermodynamic Characterization of the Multivalent Binding of Chartreusin to DNA. *Nucleic Acids Res.* **2002**, *30*, 4567−4573.
(53) Shaikh, S. A.; Ahmed, S. R.; Jayaram, B. Molecular Thermodynamic View of DNA−Drug Interactions: A Case Study of 25 minor-Groove Binders. *Arch. Biochm. Biophys.* **2004**, *429*, 81−99.